Case study for the IGS ultra-rapid orbit requirements

Jan Douša (jan.dousa@pecny.cz) Geodetic Observatory Pecný of the Research Institute of Geodesy, Topography and Cartography

The effect of ephemeris errors on PPP ZTD

Linearized equation for a carrier phase observable L_k^i (scaled to a distance) can be written as:

$$L_k^i = |\vec{R}_{k0}^i| + \Delta D_k^i + \Delta C_k^i + \Delta S_k^i + \lambda N_k^i + \epsilon_k^i \tag{1}$$

where $|\vec{R}_k^i| = |\vec{X}^i - \vec{X}_k|$ is the geometrical distance (in vacuum) between receiver k and satellite i, ΔD_k^i is the sum of the distance dependent biases (receiver and satellite position corrections, delays due to the ionosphere and troposphere), ΔC_k^i is the sum of the clock related biases (satellite and receiver clock biases, relativistic corrections), ΔS_k^i is the sum of the satellite and station dependent biases (phase center offsets and variations, multipath), λ is wavelength, N_k^i is the initial ambiguity of the full cycles in the range and ϵ_k^i is the noise.
We focus on a simplified model considering only a satellite position bias ($\Delta\vec{X}^i$) and the tropospheric path delay (ΔT_k^i) terms from a sum of distance dependent biases.

$$\Delta D_k^i = \frac{\vec{R}_{k0}^i}{|\vec{R}_{k0}^i|}\Delta\vec{X}^i - \frac{\vec{R}_{k0}^i}{|\vec{R}_{k0}^i|}\Delta\vec{X}_k + \Delta I_k^i + \Delta T_k^i \tag{2}$$

Other biases are considered as accurately provided in advance, modeled or neglected in (near) real-time analysis. Additionally, the station coordinates are usually kept fixed on a long-term estimated position (we assume $\Delta\vec{X}_k = 0$), and the ionosphere bias (ΔI_k^i) can be eliminated for its significant first order effect.
The precise satellite orbits are best estimated from a global network, while preferably kept fixed in a regional analysis, thus we consider $\Delta\vec{X}^i$ as a priori introduced error ($\delta\vec{X}^i$). In the simplest way, the troposphere parameters are estimated as the time-dependent zenith total delays (ZTD) above each station of the network

$$\Delta T_k^i = m_f(z_k^i)\cdot ZTD_k \approx \frac{1}{\cos(z_k^i)}\cdot ZTD_k \tag{3}$$

where a zenith dependent mapping function $m_f(z_k^i)$ we approximated by $\cos(z_k^i)$. Because of their different magnitude, we are interested in expressing the orbit errors in a satellite coordinate system (radial, along-track and cross-track; RAC). Using a transformation

$$\delta\vec{X}^i = R_z(\lambda^i)\cdot R_y(\varphi^i)\cdot\delta\vec{X}_{RAC}^i \tag{4}$$

we distinct only two components: radial and in orbit tangential plane (along-track + cross-track). Hence, we do not need to consider the satellite track orientation and we will investigate only the marginal errors. The equation for our simplified model is

$$L_k^i = |\vec{R}_{k0}^i| + \vec{e}_k^i\cdot R_z(\lambda^i)\cdot R_y(\varphi^i)\,\delta\vec{X}_{RAC}^i + \frac{1}{\cos(z_k^i)}\cdot ZTD_k + m_f(z_k^i)\cdot ZTD_k + \lambda\cdot N_k^i + \epsilon_k^i \tag{5}$$

where $\vec{e}_k^i$ represents a unit vector pointing from station k to satellite i. The error stemming from the orbit prediction ($\delta\vec{X}_{RAC}^i$) is usually significantly larger than the carrier phase observable noise ϵ_k^i. The orbit errors changes rather slowly (in hours) and its 3D representation is projected into the pseudorange (1D). A significant portion of this error can be mapped into the estimated ZTD if not previously absorbed by the ambiguities (or clock corrections in PPP).
For a priori orbit errors compensated mostly by ZTDs, we can write

$$\vec{e}_k^i\cdot R_z(\lambda^i)\cdot R_y(\varphi^i)\cdot\delta\vec{X}_{RAC}^i + \frac{1}{\cos(z_k^i)}\cdot\delta ZTD_k \approx 0 \tag{6}$$

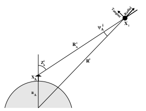

Neither the receiver position nor the velicity have to be known if we express the impact of the satellite radial and tangential errors only as a function of zenith distance to the satellite. Following the figure we express

$$\vec{e}_A^{i0}\cdot R_z(\lambda^i)\cdot R_y(\varphi^i)\cdot\delta\vec{X}_{RAC}^i = \cos(\Psi_A^i)\cdot\delta X_{Rad}^i + \sin(\Psi_A^i)\cdot\delta X_{Tan}^i \tag{7}$$

where

$$\Psi_A^i = \arcsin(\sin(z_A^i) * R_A/R^i) \tag{8}$$

and we derive the plot for the impact of the radial and tangential orbit errors to the range δL_A^i and their potential mapping into the ZTD_A.

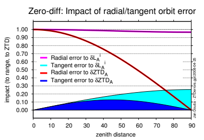

Maximal impact of the radial error is in zenith (impact 1.0). For satellite in horizon, it only slightly decreases to 0.97 for error in δL_A^i and to 0.0 for δZTD_A. The impact of the tangential errors is much smaller with maximum 0.13 at $z_k^i = 45deg$ and minimum 0.0 when tangential error is perpendicular to $\Delta\vec{X}_k^i$.
For example, $10\,cm$ tangential or $1\,cm$ radial error in orbit can cause max. $1.3\,cm$ or $1.0\,cm$ in ZTD, respectively.

Motivation

The quality of the orbits predicted for real-time plays a crutial role in the 'GPS meteorology' – precise troposphere delay estimation for the numerical weather prediction. Two approaches are commonly used: a) precise point positioning (PPP) using undifference observables and b) network solution using double-difference observables, both very different in the requirements for the orbit accuracy.
Since 2000, the International GNSS Service (IGS) provides the ultra-rapid orbits, which are updated every 6 hours today. In (near) real-time, the use of 3-10h prediction is thus necessary before getting a new IGS product.
Is the quality of current orbit prediction sufficient for 'GPS-meteorology' application ? We monitor the quality of the orbit prediction performance and relevance of the accuracy code at ***http://www.pecny.cz (GNSS → GPS-orbits)***.

The effect in the difference observables

Commonly used double-difference phase carier observations are written

$$L_{kl}^{ij} = L_{kl}^i - L_{kl}^j = (L_k^i - L_l^i) - (L_k^j - L_l^j). \tag{9}$$

This approach cancels a significant portion of common biases for two receivers or two satellites. Some biases are canceled perfectly (e.g. satellite clocks), others are more or less significantly reduced depending on baseline length (e.g. satellite position errors, troposphere path delays).
We investigate here an orbit error impact from a single satellite and thus we can use solely single-difference observations. According to (5) and (9), they are written as

$$L_{kl}^i = |\vec{R}_k^i| - |\vec{R}_l^i| + (\vec{e}_k^i - \vec{e}_l^i)\cdot\delta\vec{X}^i + m_f(z_k^i)\cdot ZTD_k - m_f(z_l^i)\cdot ZTD_l \tag{10}$$

Any orbit error is simply projected into the single-difference observation by a difference in the unit vectors $(e_k^i - e_l^i)$. If it is compensated by the difference of the estimated ZTDs (also in pseudorange projection), then

$$(\vec{e}_k^i - \vec{e}_l^i)\cdot R_z(\lambda^i)\cdot R_y(\varphi^i)\delta\vec{X}_{RAC}^i + m_f(z_k^i)\cdot\delta ZTD_k - m_f(z_l^i)\cdot\delta ZTD_l \approx 0 \tag{11}$$

We need to know the baseline length, the zenith distance of the satellite at one of the stations and the direction of the satellite with respect to the baseline. This is a bit more complicated case to generalize and we will thus study its two marginal cases which both meet in the zenith above the mid of a baseline:

- ***equal azimuths*** - satellite and second station are in equal azimuths
- ***equal zeniths*** - zeniths to satellite are equal for both stations

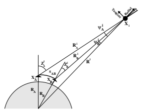

Again, we do not need to know the satellite velocity vector if we distiguish the ephemeris errors only in radial and tangential direction, but baseline lenght is still necessary. According to (7), (8) and (10), we get a relation for the impact (12) which is evaluated for two cases above and the baseline $S_{AB} = 1000km$) in the plots.

$$(\vec{e}_A^i - \vec{e}_A^i)\cdot R_z(\lambda^i)\cdot R_y(\varphi^i)\cdot\delta\vec{X}_{RAC}^i = (\cos(\Psi_A^i)\cdot\delta X_{Rad}^i + \sin(\Psi_A^i)\cdot\delta X_{Tan}^i) - (\cos(\Psi_B^i)\cdot\delta X_{Rad}^i + \sin(\Psi_B^i)\cdot\delta X_{Tan}^i) \tag{12}$$

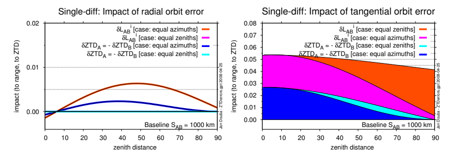

In case of equal zeniths ($z_A^i = z_B^i,\ R_A^i = R_B^i,\ \Psi_A^i = \Psi_B^i$), the impact is always canceled out for the radial orbit error. Tangential orbit error has maximal impact when the satellite is above the baseline and the error is parallel with baseline (± 0.027 for ZTD_A, ZTD_B). It is cancelled out when the error is perpendicular to the baseline and reduced to the horizon. In case of equal azimuths, the impact of the radial orbit error is maximal at $z_A^i = 38\ deg$ (± 0.0023 for ZTD_A, ZTD_B respectively). Tangential error impact is the largest again above the baseline (the same as in equal zenith case) and slightly faster reduces to the horizon. The impact is reduced with decreasing the baseline length (approx. half for baseline $500km$).

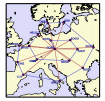

Simulation in network analysis

We used a network solution processed with the Bernese GPS software to simulate the Radial/Along-track/Cross-track (RAC) orbit errors. The ZTDs were estimated using 'star' and 'circle' networks with the longest baseline of $1300km$ ('star'). The precise IGS final orbits were used for data pre-processing, ambiguity fixing, for estimating the reference coordinates and ZTDs. The synthetic biases ($1cm - 100cm$) were introduced into the IGS final orbits successively for G01, G03, G05 and G25 satellite in the RAC components independently. Two ZTD solutions were provided and compared to the reference ZTDs – ambiguity fixed (top Figs) and ambiguity free (bottom Figs). The ZTD map differences are plotted for radial, along-track and cross-track components in a 3-hr interval when satellite is above the region (Figs below).

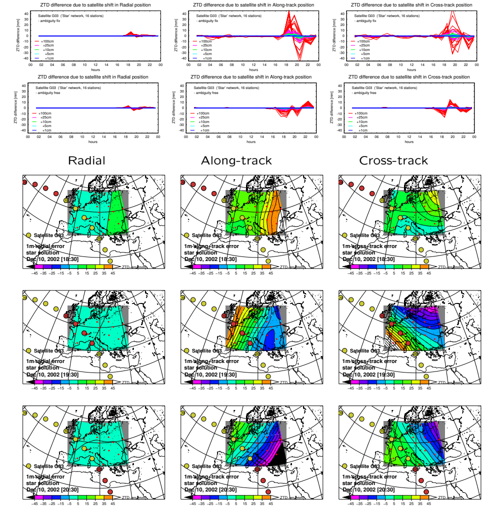

Summary

	Radial	Tangent
PPP	1 cm	7 cm
Network	217 cm	19 cm

The table shows the example requirements for the radial and tangential orbit position accuracy to ensure that the ZTD contamination is lower than $1cm$ (when not absorbed by the ambiguities or clock corrections). In a network, we consider $1000km$ baselines (the effects will reduce to one-half in case of $500km$ baselines). Because the ambiguities are able to absorb a significant portion of the ephemeris errors in both cases, they help to overcome the current deficiencies in predicted orbit quality. To set up general requirements is difficult - the satellite constellation, the network configuration and especially the pre-processing (solving for ambiguities, clocks, coordinates) altogether differentiate the situation in which the orbit errors can be absorbed into different model constituents. The radial component errors are negligible in the network solution, but the most inaccurate orbit along-track component can ocassional affect the ZTDs when the satellite is flying in a baseline direction. Only some of the baselines are sensitive in specific situations and, unfortunately, the averaging, with respect to other satellite observables, is thus limited. The radial component is crucial in PPP ZTDs when satellite is near the zenith, while the along-track component causes maximal error in elevation of $45deg$ if the satellite is flying to or from the station. Fortunately, the error averaging performs over all the satellites. Satellite clock corrections can additionally absorb a significant part of the error in the regional solution. Usually, only a few weakly estimated satellites occur in a single product, thus a robust satellite checking strategy applied by the user will be satisfactory in many cases for the network solution. A significantly different pattern of the orbit accuracy degradation, with respect to the prediction time, is clearly identified for the GPS Block IIR and IIA satellites during an eclipsing period. There are 14 (15) of IIA satellites from the whole GPS constellation (including PRN32) and they still represent 44%. The accuracy codes are in most cases relevant, but usually underestimated for the Block-IIA satellites during the eclipsing periods and at the beginning of the maintenance periods.

Monitoring the quality of the IGS ultra-rapids

The overall accuracy of the precise IGS ultra-rapid orbit product is usually presented by means of weighted rms. We present a detail evaluation with respect to each individual satellite and with respect to every hour of 0-24h interval prediction. The aim is to evaluate the individual satellite orbit quality and assigned accuracy codes separately.
The IGS ultra-rapid orbits are epoch by epoch compared to the IGS rapid product (3 rotations estimated for every epoch). From the differences, which are stored in a database we generate the plots of

- the orbit accuracy dependency on the prediction interval (Fig 1),
- the evolution of the individual orbit accuracy in the time-series (Fig 2),
- to monitor the real orbit differences together with the triple of expected error assigned to satellite ($3 * 2^{AccCode}$) (Fig 3).

The Figure 4 finally shows 1D RMS from the IGS ultra-rapid comparison to IGS rapids provided by the IGS ACC, which display in yellow the eclipsing periods clearly identifying the problems in specific satellite predictions.

Figure 1

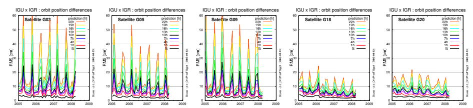

Figure 2

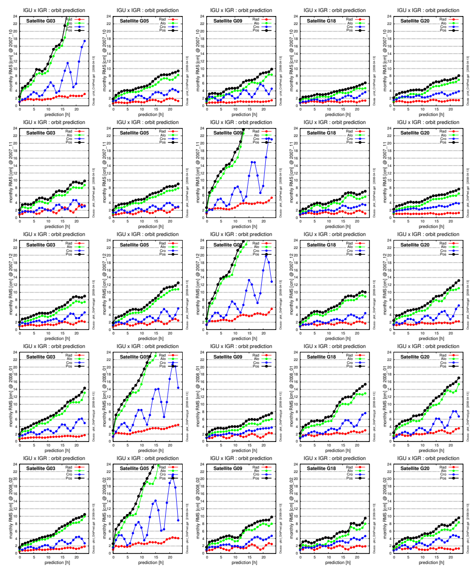

Figure 3

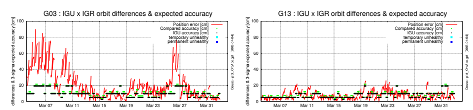

Figure 4

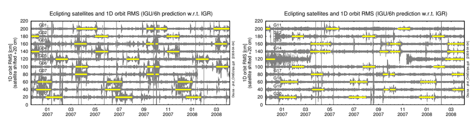

Acknowledgement: Support of the Czech Science Foundation 205/09/0696.